ISSN 2359-4799
Volume 11 / Number 1 / Year 2025 – p. 01-26
DOI: 10.36524/ric.v11i1.3144

GRAPHICAL ABSTRACT

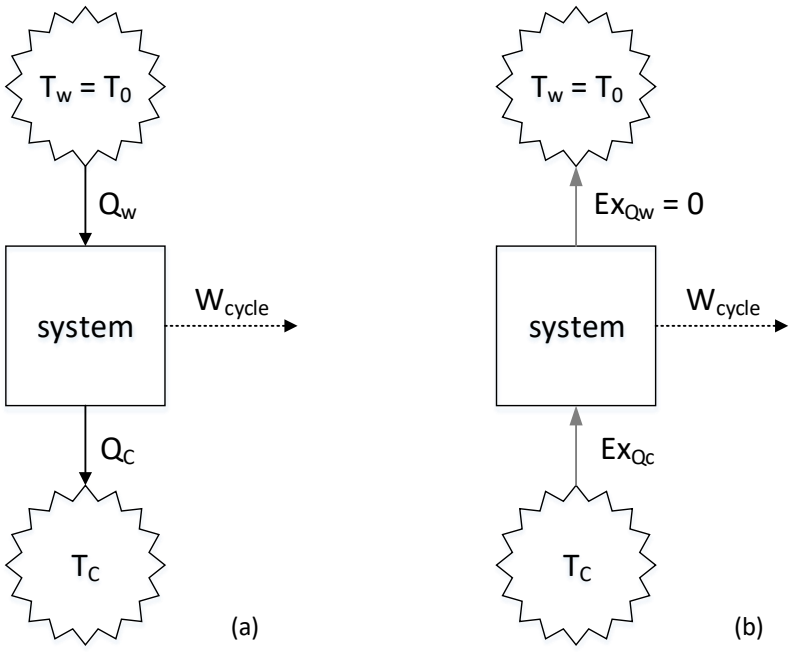

Schematic diagrams of power cycles when the reference temperature equals the warm surface water temperature: (a) energy transfers, (b) exergy transfers

STANDARDIZATION PROPOSAL FOR EXERGY ANALYSIS OF OCEAN THERMAL ENERGY CONVERSION POWER CYCLES

Atilio Barbosa Lourenço [1]*

[1]Departamento de Engenharia Mecânica, Universidade Federal do Espírito Santo, Avenida Fernando Ferrari, 514 – Goiabeiras CEP 29075-910 – Vitória – ES – Brasil

* (atilio.lourenco@ufes.br)

Article submitted in 19/02/2025, accepted in 03/04/2025 and published in 26/05/2025.

ORCID – Atilio Lourenço: https://orcid.org/0000-0003-3375-6237

Abstract: There is a need to reduce carbon dioxide emissions to mitigate the effects of climate change. One of the solutions lies in ocean thermal energy conversion (OTEC) systems. When reviewing the literature, it is evident that the exergy analysis of these systems does not follow any established standard. Therefore, a standard is proposed in this work: to consider the reference environment temperature as the temperature of the warm surface water and associate the cold deep-water temperature with the exergy input of the cycles. Firstly, reversible power cycles are studied. Subsequently, an organic Rankine cycle (ORC) is analyzed. Approaches found in the literature are also applied to analyze the ORC. It is shown that, for any reversible power cycle, when the hot reservoir temperature equals the reference environment temperature, the work produced by the cycle equals the exergy accompanying the heat transfer associated with the cold reservoir temperature. For an ORC, taking the reference environment temperature as the warm surface water temperature and considering the exergy input as the exergy change of the deep cold water in the condenser generates robust and coherent results. The proposed standard can contribute to the systematic advancement of scientific knowledge on OTEC systems.

Keywords: engineering thermodynamics; exergetic efficiency; ORC; OTEC; second law analysis.

1 INTRODUCTION

The world is facing a catastrophic period concerning the environment. Climate change is a reality, and humanity must act to, at the very least, mitigate the effects of these changes. Science has shown that increasing carbon dioxide sinks and reducing sources of this gas are urgent actions that must be taken. Regarding emissions, electricity generation from fossil energy sources is among the main contributors. Due to this, the world is undergoing an energy transition aimed at decarbonization.

Renewable energy sources have been employed in the energy transition. Solar, wind, biomass, and geothermal energy have been applied, and their technologies are continuously being developed. The utilization of waste, whether organic waste or residual heat, for electricity generation has also gained prominence.

Regarding renewable sources, there is also a focus on the oceans. Systems to convert energy from waves and tides have been proposed. Additionally, the oceans hold potential for electricity generation due to the temperature gradient that exists in the vertical direction. To exploit this potential, ocean thermal energy conversion (OTEC) systems have been proposed. Despite the high cost of implementation, a relevant feature of these systems is that they offer superior stability compared to solar and wind energy systems (Xiao and Gulfam 2023).

For the performance evaluation of energy conversion systems, including OTEC, a widely used tool is exergy analysis. The main objective is to identify, in light of the second law of thermodynamics, the inefficiencies in the thermodynamic processes associated with the system's components. Based on the results of this analysis, decisions can be made for resource conservation (de Oliveira Junior 2013).

There are dozens of published studies on the exergy analysis of OTEC systems or energetically integrated systems that include an OTEC power cycle. Despite the notable efforts of researchers to analyze such systems, aiming for improvements or optimization, there is no standard regarding the definition of fundamental information to carry out the exergy analysis. Thus, the comparison of results from different studies is weakened.

Table 1 presents citations of studies that employed exergy analysis on systems composed of OTEC. The selected and presented information includes the warm surface ocean water temperature, the reference environment temperature, and the definition of exergy input for the calculation of exergetic efficiency of the power cycle. In general, it is possible to see that not all three selected pieces of information are always available. Furthermore, it can be observed that the choice of the reference environment temperature does not correspond to T_W except in four studies. Additionally, there is no single definition of exergy input and, consequently, of the calculation of exergetic efficiency. It is emphasized that net exergy refers to the exergy change of a material flow passing through a heat exchanger, while gross exergy is the flow exergy at a specific point.

Table 1: Temperatures of warm water, reference environment, and exergy inputs

Study	T_w	T_0	Exergy input
Yilmaz (2019)	30–35 °C	20 °C	Net exergy of the water entering the evaporator.
Malik et al. (2020)	<24–30 °C	-	Gross exergy of the water entering the evaporator and condenser.
Ahmadi et al. (2013)	22 °C	25 °C	Gross exergy of the water entering the evaporator and condenser.

Yoon et al. (2013)	25 °C	30 °C	Exergy associated with the heat entering the evaporator.
Talluri et al. (2021)	29.56 °C	15 °C	-
Ma et al. (2022)	28 °C	-	-
Ishaq et al. (2019)	28 °C	25 °C	Gross exergy of the water entering the evaporator and condenser.
Sun et al. (2012)	25–31 °C	20 °C	Gross exergy of the water entering the evaporator and condenser.
Gao et al. (2024)	31 °C	35 °C	Net exergy of the water entering the evaporator, superheater, and condenser, as well as the power of the pump and expander.
Haroon et al. (2022)	28 °C	10 °C	Exergy associated with the heat entering the evaporator.
Basta et al. (2021)	29.6 °C	-	Net exergy of the water entering the evaporator and condenser.
Chen et al. (2016)	27–31 °C	-	-
Jung et al. (2016)	26.19 °C	-40 °C	Net exergy of the water entering the evaporator.
Yasunaga et al. (2021)	29–31 °C	-	A mathematical expression as a function of the mass flow rates, specific heats, and temperatures of the water entering the evaporator and condenser.
Ofosu-Adarkwa and Hao (2017)	25–40 °C	25 °C	Net exergy of the water entering the evaporator.
Doorga et al. (2018)	25 °C	5 °C	Exergy associated with the heat entering the evaporator.
Zhou et al. (2020)	29 °C	25 °C	Net exergy of the water entering the evaporator.
Zhu et al. (2022)	29 °C	25 °C	Net exergy of the water entering the evaporator and condenser.
Du et al. (2024)	25 °C	T_W	-
Khanmohammadi et al. (2020)	23 °C	20 °C	Exergy associated with the solar heat entering the collector.
Hernández-Romero et al. (2020)	24–31 °C	25 °C	Gross exergy of the water entering the evaporator and condenser, and exergy associated with the solar collector.
Hasan and Dincer (2020)	26 °C	4.5 °C	Exergy associated with the heat entering the evaporator.
Khosravi et al. (2019)	27 °C	20 °C	Gross exergy of the water entering the evaporator and condenser.
Zhou et al. (2021)	29 °C	25 °C	Net exergy of the water entering the evaporator.
Zhang et al. (2022)	27–32 °C	20 °C	Net exergy of the water entering the evaporator.
Ma et al. (2024)	28 °C	5 °C	Net exergy of the water entering the evaporator.
Hoseinzadeh et al. (2024)	27.5 °C	25 °C	Gross exergy of the water entering the evaporator, condenser, and power of the pump.
Hoseinzadeh et al. (2023)	30 °C	25 °C	Exergy associated with solar radiation.

Kim et al. (2017)	28 °C	20 °C	Exergy associated with the heat entering the evaporator, using the cold-water temperature as the reference temperature.
Wang et al. (2018)	22–27 °C	20 °C	Gross exergy of the water entering the evaporator, condenser, and power of the pump.
Langer et al. (2022)	23.7–29.2 °C	6–9 °C	Gross exergy of the water entering the evaporator.
Colorado-Garrido et al. (2024)	28 °C	0 °C	Net exergy of the water entering the evaporator.
Zhang et al. (2024)	26–31 °C	35 °C	Net exergy of the water entering the evaporator and superheater.
Huo et al. (2023)	30 °C	T_W	Net exergy of the water entering the evaporator and superheater.
Fan et al. (2024)	28 °C	-	Net exergy of the water entering the evaporator and superheater.
Zhang et al. (2024)	22–34 °C	-52 °C	Exergy associated with the heat leaving the condenser.
Dezhdar et al. (2023)	30 °C	25 °C	Exergy associated with solar radiation.
Zhang et al. (2023)	20–35 °C	T_W	Exergy associated with the heat entering the generator and leaving the condenser.
Yilmaz et al. (2024)	28–38 °C	25 °C	Net exergy of the water entering the evaporator.
Soyturk and Kizilkan (2024)	21–28 °C	20 °C	Gross exergy of the water entering the evaporator.
Zoghi et al. (2024)	22–36 °C	20 °C	Gross exergy of the water entering the evaporator and condenser, and exergy associated with the solar collector.
Zainul et al. (2024)	30 °C	25 °C	-
Ishaq and Dincer (2020)	28 °C	0–30 °C	Gross exergy of the water entering the evaporator and condenser.
Tian et al. (2023)	30 °C	15 °C	Net exergy of the water entering the evaporator and condenser, and the power of the pump.
Yuan et al. (2015)	26 °C	25 °C	Exergy associated with the heat entering the generator.
Yilmaz et al. (2018)	10–40 °C	0–40 °C	Net exergy of the water entering the evaporator.
Xiao et al. (2024)	30 °C	6 °C	Net exergy of the water entering the evaporator.
Geng and Gao (2023)	25 °C	T_W	Gross exergy of the water exiting the auxiliary heat subsystem.
Assareh et al. (2021)	30 °C	25 °C	Exergy associated with the solar collector and gross exergy of the warm surface water.
Azhar et al. (2017)	28 °C	15–25 °C	Net exergy of the water entering the evaporator.
Yuan et al. (2014)	28–33 °C	25 °C	Exergy associated with the heat entering the generators and reheater.

Ahmadi et al. (2015)	-	25 °C	Gross exergy of the water entering the evaporator and condenser, and exergy associated with the solar collector.
Sun et al. (2017)	25 °C	20 °C	Exergy associated with solar radiation.
Bahari et al. (2024)	30 °C	25 °C	Exergy associated with solar radiation.

Source: The author.

The organic Rankine cycle (ORC), with or without modifications, was the system chosen in most of the cited studies. In Basta et al. (2021), Du et al. (2024), and Xiao et al. (2024), the Kalina cycle was studied. In Ofosu-Adarkwa and Hao (2017), the Goswami cycle was analyzed. In Zhu et al. (2022), the Uehara cycle was evaluated. Fan et al. (2024) separately assessed the Organic Rankine Cycle and the Kalina cycle. Zhang et al. (2023), Yuan et al. (2015), and Yuan et al. (2014) studied cycles with ejectors.

One study not cited in Table 1 is the work published by Yasunaga et al. (2021). A definition for the reference environment temperature is proposed, which is the equilibrium temperature between the warm water from the evaporator and the cold water from the condenser, according to their respective mass flow rates, specific heats, and temperatures. This approach could have physical meaning if, for example, both flows were intended for an insulated mixing tank. Alternatively, it could have physical significance if the flows were discharged at the depth corresponding to that temperature. However, in real systems, this is not the case. The intake of warm water occurs at approximately 20 meters depth. To avoid discharging warm water and minimize the environmental impacts of this water returning to the ocean, it is sufficient for the outflow streams to be discharged at approximately 60 meters depth (Vega 2012). On the other hand, there is data showing that the average depth of the ocean's isothermal layer is increasing over time (Chu and Fan 2020). As of 2017, the average depth of the isothermal layer was 67.5 m, meaning that up to this depth, the water temperature can be considered constant from the ocean's surface.

In Yasunaga and Ikegami (2020), a similar approach was applied. The reference environment temperature was interpreted as the equilibrium temperature at which both reservoirs of warm water and cold water would be found. This situation was defined as "the dead state of OTEC."

Another article not cited in Table 1 is the one written by Fachina (2016). In this article, the possibility of using an OTEC system to supply a seawater desalination system in the context of the northeastern region of Brazil is analyzed. Although not applied in the proposed modeling, the concept of exergy is discussed. The temperature of the cold water was taken as the reference environment temperature. In this case, the exergy of the warm surface water was calculated.

In light of the above, the objective of this work is to propose and evaluate a standard for the exergy analysis of OTEC power cycles: to take the reference environment temperature as the temperature of the warm surface water and associate the temperature of the cold deep water with the exergy input of the cycles. It is understood that the warm surface water of the oceans, which represents the local physical environment, corresponds to the reference environment, while the cold deep water is the material resource to be obtained from the effort, similar to geothermal energy, solar energy, etc., in conventional power systems.

There are two novelties presented in this work. First, it involves the proposal of the standard itself and its application to an OTEC system based on ORC. As shown in

Table 1, there are no published studies with this approach. Additionally, an exergetic study is conducted on reversible power cycles that operate below the reference environment temperature. Even basic thermodynamics textbooks do not address this topic.

This work contributes to the systematic advancement of scientific knowledge regarding OTEC systems. Based on the standard proposed in this work, the comparison of results from different studies can be made consistently. This could support the advancement of the implementation of OTEC systems.

2 MATERIALS AND METHODS

Two types of systems are addressed from an exergetic perspective in this work. First, reversible power cycles are analyzed. Subsequently, an ORC is examined, as it is the most analyzed type of OTEC system for electricity generation according to the literature. All models are simulated using the Engineering Equation Solver computational software (F-Chart Software 2017).

2.1 REVERSIBLE POWER CYCLES

Reversible power cycles are theoretical cycles that do not present internal or external irreversibilities in their operation. Thus, these cycles can be interpreted as a perfect model of real power systems based on thermodynamic cycles, serving as a reference model. Therefore, it is necessary to start the analysis with theoretical cycles before proceeding to real systems, such as the ORC.

As real power systems usually operate at temperatures above the reference environment temperature, generally taken as the air temperature, the typical model for reversible cycles follows the logic of setting the cold reservoir temperature equal to the environment temperature. From an exergetic perspective, an example can be found in a citation from the textbook by Çengel et al. (2023):

> For a heat engine, the exergy expended is the decrease in the exergy of the heat transferred to the engine, which is the difference between the exergy of the heat supplied and the exergy of the heat rejected. (The exergy of the heat rejected at the temperature of the surroundings is zero.) The net work output is the recovered exergy.

In this work, it is proposed to set the hot reservoir temperature equal to the environment temperature, that is, the temperature of the warm surface water. Figure 1 illustrates two schematic diagrams of a reversible power cycle, one showing energy transfers and the other showing exergy transfers. As $T_W > T_C$, from an energy perspective, nothing changes compared to what is already known. However, from an exergetic perspective, the exergy input is associated with the cold reservoir. Additionally, since $T_W = T_0$, the exergy transferred to the hot reservoir is zero. As the cycle is reversible, the work generated by the cycle must be equal to the exergy input. The demonstration of this statement is available in Appendix A.

Figure 1: Schematic diagrams of a reversible power cycle: (a) energy transfers, (b) exergy transfers

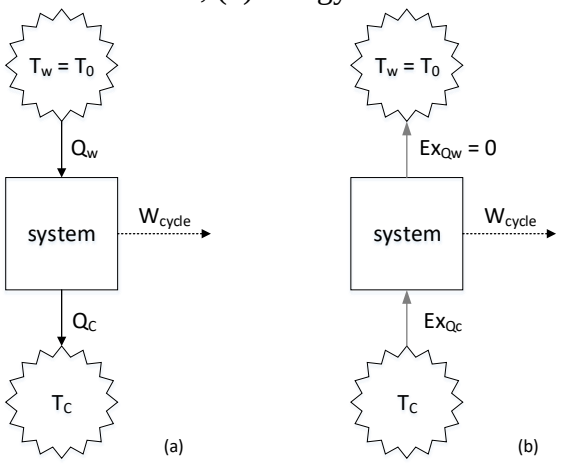

Source: The author.

To enhance the consistency of the proposed approach, specific cycles are

analyzed. Basic thermodynamics textbooks, such as Çengel et al. (2023) and Moran et al. (2018), indicate that there are specifically three reversible power cycles: the Carnot, Stirling, and Ericsson cycles.

The four processes that make up the Carnot cycle are isentropic expansion, isothermal heat rejection at T_C, isentropic compression, and isothermal heat addition at T_W. The other two cycles differ from the Carnot cycle because there are no isentropic processes. In the Stirling cycle, these processes are replaced by isochoric regeneration processes. In the Ericsson cycle, there are two isobaric regeneration processes. Regeneration is the internal heat transfer from the working fluid to a thermal energy storage in one process, followed by the internal heat transfer from the storage back to the working fluid in another process.

The *P*-*v* and *T*-*s* diagrams of the cycles are presented in Figure 2. For the Stirling and Ericsson cycles, the working fluid is modeled as an ideal gas. This is not the case, however, for the Carnot cycle. The adoption of a real fluid, with phase change occurring during the cycle, is due to its association with what happens in real systems, such as the ORC. Nevertheless, there is no loss of generality in the proposed approach if an ideal gas were adopted for the Carnot cycle. All cycles can be analyzed from the perspective of a closed system or as control volumes operating under steady-state conditions. Therefore, there is a combination of six cycles.

Equations 1 and 2 represent the energy balance per unit mass for a closed system and for a control volume, respectively. The work per unit mass for a closed system and for a control volume can be calculated according to Equations 3 and 4, respectively. It is emphasized that the expressions are presented according to the sign convention. With the results of the energy balances, the net amount of work per unit mass exchanged between the system and its surroundings can be accounted for. This amount must be equal to the specific exergy associated with the heat transfer at T_C.

$$q_{CS} - w_{CS} = \Delta u \quad (1)$$

$$q_{CV} - w_{CV} = \Delta h \quad (2)$$

$$w_{CS} = \int P\, dv \quad (3)$$

$$w_{CV} = -\int v\, dP \quad (4)$$

Table 2 presents the input data for the baseline cases. The temperature of the cold water at a depth of 1 km was obtained from Xiao and Gulfam (2023) and is taken here as T_C. The values of *CR* for the Stirling cycle, *PR* for the Ericsson cycle, and P_1 for both cycles are arbitrarily chosen. The temperature of the warm surface water is also arbitrarily determined. It is emphasized that a parametric analysis will be conducted later.

For OTEC based on ORC, Bernardoni et al. (2019) showed that the best economic performance was achieved using ammonia, R-32, and propylene. Therefore, these are the fluids chosen for the Carnot cycle. Katooli et al. (2020) simulated a real Stirling engine considering three different fluids, namely helium, nitrogen, and hydrogen. Thus, these gases are also considered for the Stirling cycle. The three gases adopted for the Ericsson cycle are the same as those for the Stirling cycle. This approach was utilized by Costa and MacDonald (2018) and is applied here as well.

2.2 ORGANIC RANKINE CYCLE

Figure 3 shows the schematic diagram of the analyzed ORC. The gray arrows indicate the working fluid. The ocean water is represented by the dashed black arrows. Power is transferred according to the solid black arrows. The difference between the power produced by the turbine and the power demanded by the pump flows to the surroundings of the cycle, with the circle representing a power distributor. An electric generator is coupled

to the turbine shaft, and an electric motor drives the pump. The working fluid is vaporized in the evaporator and directed to the turbine. Power is generated, and the working fluid exits the turbine to be condensed in the condenser. The pump draws liquid from the condenser and pumps this pressurized liquid to the evaporator. The warm surface water interacts with the evaporator, while the cold deep water exchanges heat with the condenser. The ocean water pumps are not taken into account because the focus is on the analysis of the cycle itself. However, this does not affect the arguments presented in this work if such pumps were to be considered.

Figure 2: *P*-*v* and *T*-*s* diagrams of the (a) Carnot, (b) Stirling, and (c) Ericsson cycles

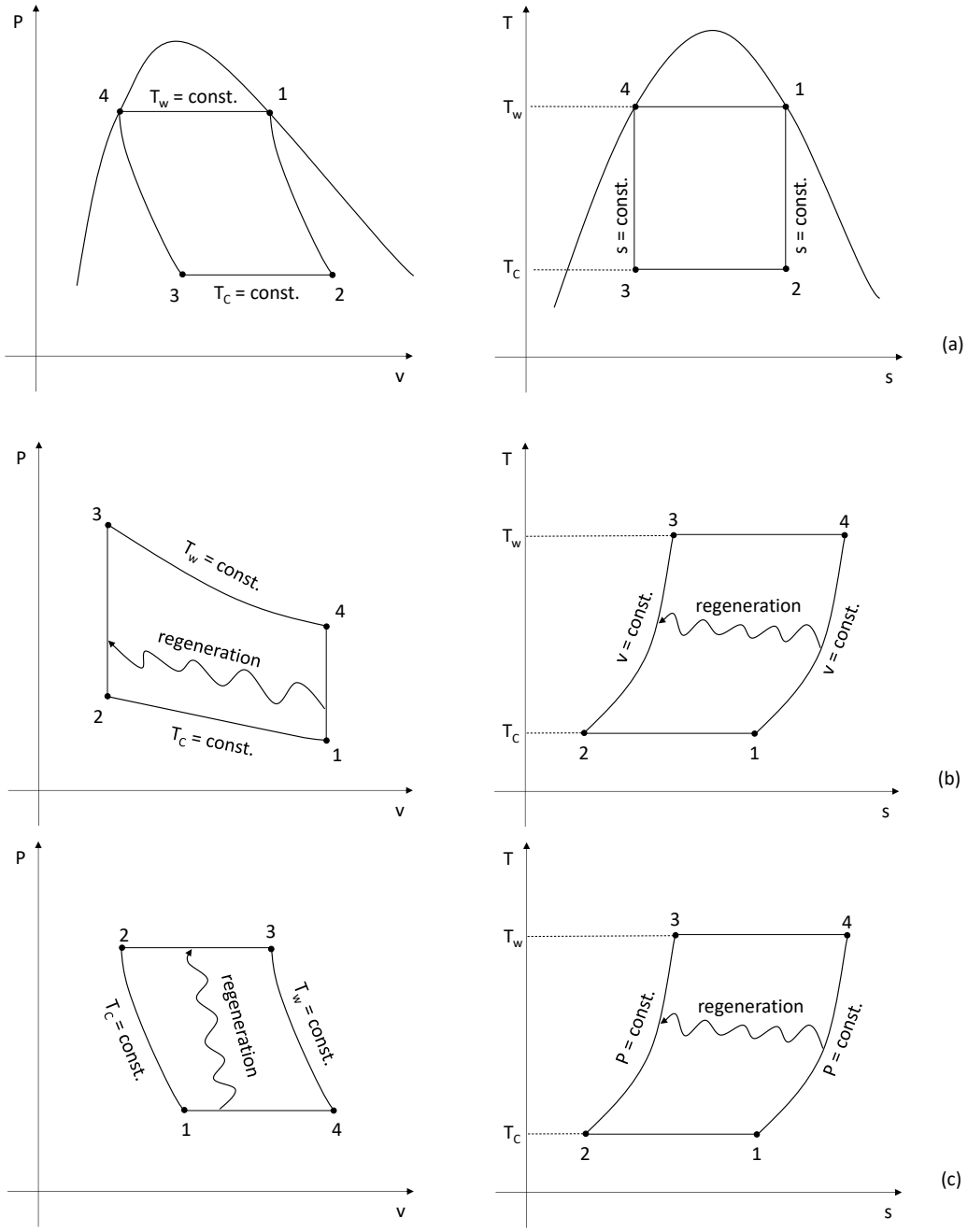

Source: The author.

Table 2: Input data for the reversible cycles for the baseline cases

Parameter	Carnot	Stirling	Ericsson
P_0 [kPa]	-	101.325	101.325
T_0 [°C]	25	25	25
T_C [°C]	4	4	4
$CR = v_1/v_2$	-	3	-
$PR = P_3/P_2$	-	-	3
P_1	-	P_0	P_0

Source: The author.

Figure 3: Schematic diagram of the ORC

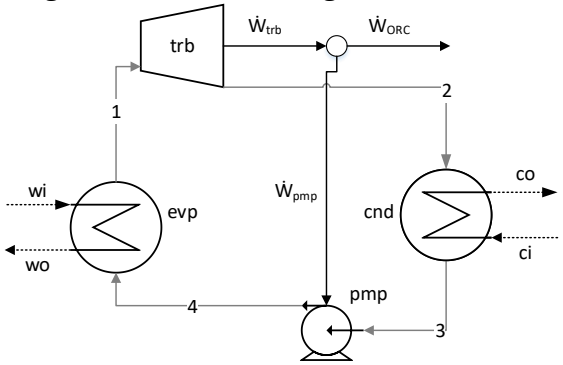

Source: The author.

The assumptions for modeling the ORC are listed below:

- The components of the cycle operate under steady-state conditions.
- There is no significant heat loss in the cycle components.
- Kinetic and potential energy changes are neglected.
- There is no significant pressure drop in the heat exchangers.
- Saturated vapor exits the evaporator.
- Saturated liquid exits the condenser.
- Ocean water is considered as pure water in the saturated liquid state.

The temperature distributions in the evaporator and condenser are graphically represented in Figure 4. In the analyzed ORC, there is superheated vapor at the condenser inlet and compressed liquid at the evaporator inlet. Thus, the pinch points of the heat exchangers must be considered for the modeling to be consistent.

Figure 4: Graphical representation of the temperature distributions in the evaporator and condenser

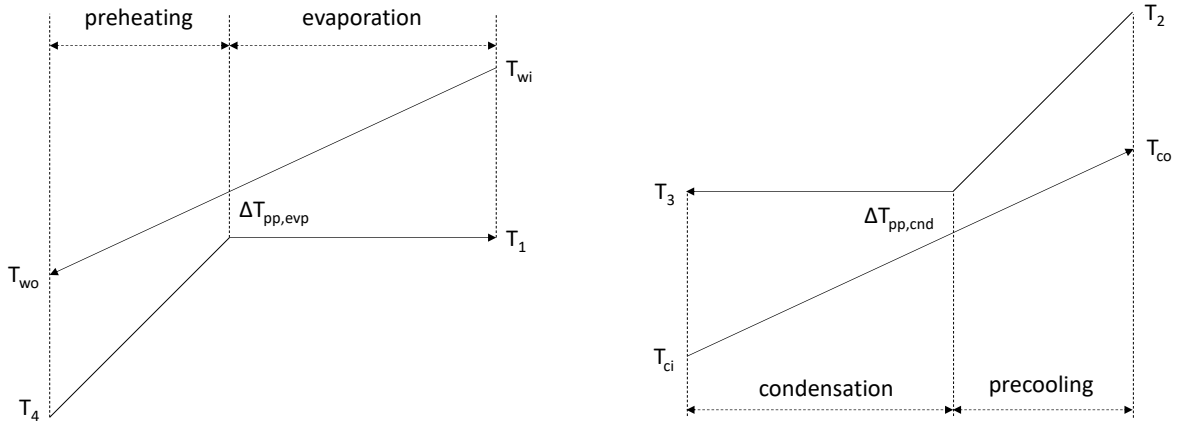

Source: The author.

The energy and exergy balance equations for each component of the cycle are written according to Equations 5 and 6, with the change in the exergy rate of the material streams calculated according to Equation 7. The unit of T_0 must be in Kelvin (K). The fractions of exergy destruction and loss relative to the exergy input of the ORC are defined according to Equations 8 and 9. The exergetic efficiency of the ORC is calculated using Equation 10.

$$0 = -\dot{W} + \sum \dot{m}_i (h_i - h_o) \quad (5)$$

$$0 = -\dot{W} + \sum \left(\dot{E}x_{f,i} - \dot{E}x_{f,o} \right) - \dot{E}x_D \quad (6)$$

$$\dot{E}x_{f,i} - \dot{E}x_{f,o} = \dot{m}_i [h_i - h_o - T_0 (s_i - s_o)] \quad (7)$$

$$y_D = \frac{\dot{E}x_D}{\dot{E}x_{i,ORC}} \quad (8)$$

$$y_L = \frac{\dot{E}x_L}{\dot{E}x_{i,ORC}} \quad (9)$$

$$\varepsilon_{ORC} = \frac{\dot{W}_{ORC}}{\dot{E}x_{i,ORC}} \quad (10)$$

To better assess the proposed standard, three definitions for the exergy analysis of the ORC are applied. In each definition, a reference environment temperature and an exergy input are adopted. Definition 1 is associated with the proposed standard. The net exergy of the condenser water enters the cycle. Part of it is destroyed in the four components of the ORC. Another part is converted into net power. The remainder is lost with the evaporator water, represented by the net exergy of that water.

In Definition 2, it is ensured that there is a reduction in the net exergy of the evaporator and condenser water. A temperature of 5°C below T_{wo} is arbitrarily chosen. However, there is no loss of generality in the arguments presented, as long as $T_0 > T_{co}$. For Definition 2, there is no exergy lost to the surroundings of the ORC.

For Definition 3, the ORC is treated conventionally, that is, like ORCs that operate at temperatures above the reference environment temperature (air). The net exergy of the evaporator water feeds the ORC, with part of it being destroyed in the cycle components, another part converted into net power, and the remainder lost to the surroundings of the ORC via the condenser water.

The three definitions are listed in Table 3. In all definitions, the gross exergy of the water entering the evaporator and/or condenser is not considered. From a rational perspective, the net exergies of the water are the exergies associated with the operation of the cycle itself. Additionally, a definition with $T_0 < T_{wo}$ and with the exergy input equal to the net exergy of the water entering the evaporator is not considered, as inconsistent results are obtained from such a definition. Nevertheless, for informational purposes, the simulation results considering this definition are presented in Appendix B.

Table 3: Definitions for the exergy analysis of the ORC

Definition	T_0	Exergy input
1	T_{wi}	Net exergy of the water entering the condenser.
2	T_{wo} - 5°C	Net exergy of the water entering the evaporator and condenser.
3	T_{ci}	Net exergy of the water entering the evaporator.

Source: The author.

The input data for the ORC simulations are presented in Table 4. All data were obtained from the optimized ORC, whose working fluid is R-134a, as reported by Yang et al. (2022).

Table 4: Input data for the ORC simulations

Parameter	Amount
$\dot{m}_{R\text{-}134a}$	7.117 kg/s
η_{trb}	0.80
η_{pmp}	0.60
τ_{gen}	0.90
τ_{mtr}	0.90
T_{wi}	28°C
T_{ci}	4 °C
T_{evp}	23.24 °C
T_{cnd}	11.50 °C
$\Delta T_{pp,evp}$	1.48 °C
$\Delta T_{pp,cnd}$	1.78 °C

Source: The author.

Only for Definition 1, a parametric analysis is conducted to obtain generalized information about the thermodynamic

robustness of the proposed standard. The influence of the pinch points of the two heat exchangers and the isentropic efficiencies of the two machines on the respective rates of exergy destruction and fractions of exergy destruction is analyzed.

3 RESULTS AND DISCUSSION

The results of the simulations for the baseline cases and the parametric study are presented and discussed for the reversible power cycles. For the ORC, the results of the simulations for the three definitions and the parametric analysis of the definition corresponding to the proposed standard are shown.

3.1 REVERSIBLE POWER CYCLES

Table 5 presents the amounts of work per unit mass for each process and for the cycle, as well as the amounts of heat per unit mass entering and leaving the system. The specific exergy associated with the heat transfer related to T_C is also presented. The working fluids considered are ammonia and helium. The amounts shown in the table can aid in the reproducibility of the results. As expected, the net work per unit mass and the specific exergy associated with the heat transfer related to T_C are the same for all cycles.

Table 5: Results for the baseline cases of the reversible power cycles

Amount [kJ/kg]	Carnot, CS	Carnot, CV	Stirling, CS	Stirling, CV	Ericsson, CS	Ericsson, CV
q_w	1165.9	1165.9	680.3	680.3	680.3	680.3
q_c	-1083.8	-1083.8	-632.4	-632.4	-632.4	-632.4
$w_{1.4}$	126.8	0	0	43.6	680.3	680.3
$w_{2.1}$	76.2	86.5	-632.4	-632.4	-43.6	0
$w_{3.2}$	-108.0	0	0	-43.6	-632.4	-632.4
$w_{4.3}$	-12.9	-4.4	680.3	680.3	43.6	0
w_{cycle}	82.1	82.1	47.9	47.9	47.9	47.9
ex_{qc}	82.1	82.1	47.9	47.9	47.9	47.9

Source: The author.

Figure 5 shows the parametric curves as a function of the reference environment temperature for the Carnot cycle, considering both the closed system and control volume approaches. For the three working fluids considered, and as expected, the net work per unit mass is equal to the specific exergy associated with the heat transfer related to T_C, regardless of T_0. Also as expected, the higher the T_0, the higher the input exergy, as the temperature difference between the thermal reservoirs increases as well.

Figure 6 illustrates the parametric curves as a function of the reference environment temperature, compression ratio, and pressure at state 1 for the Stirling cycle. Again, this result applies to both the closed system and control volume approaches. The same discussion regarding T_0 for the Carnot cycle can be applied to the Stirling cycle. Additionally, the higher the *CR*, the more heat per unit mass is exchanged between the system and its surroundings, resulting in a higher exergy input. On the other hand, P_1 has no effect on this variable.

For the Ericsson cycle, the same discussion regarding the Stirling cycle results can be applied by simply replacing *CR* with *PR*. Thus, Figure 6 also presents the results for the Ericsson cycle.

3.2 ORGANIC RANKINE CYCLE

The pressures and temperatures of R-134a obtained in the reference study by Yang et al. (2022) and in the present study are shown in Table 6. All the properties

obtained deviate very little from those obtained in the reference study. Thus, it is understood that the thermodynamic model of the ORC is validated.

Table 7 presents the mass flow rates, specific enthalpies, and specific entropies of the R-134a and water streams. The amounts shown in the table can aid in the reproducibility of the results.

Figure 5: Parametric curves as a function of T_0 for the Carnot cycle

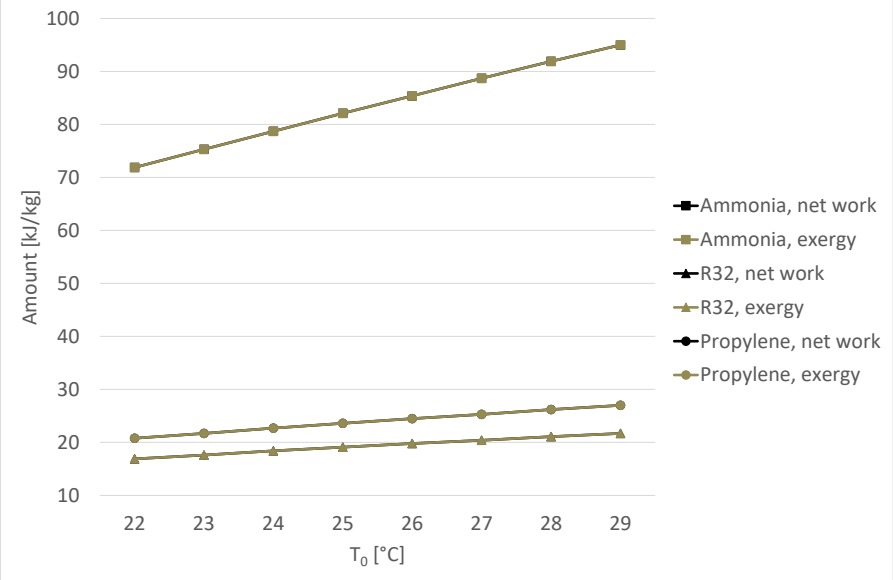

Source: The author.

The exergy balance sheets for the three definitions are shown in Table 8. The total exergy input must be equal to the sum of the net power and the exergy destructions and losses. The percentages in parentheses are associated with exergetic efficiency and exergy destructions and losses. It is clearly seen that the results generated by the three definitions are different.

Regardless of the adopted definition, the net power is the same. This is expected since the power generated by the ORC is obtained through the energy modeling of the cycle, which does not depend on second law considerations.

For all ORC components, the exergy destruction rates decrease as T_0 decreases. This is also expected, as it is consistent with the Gouy-Stodola theorem. The exergy destruction rate can be calculated as the product of T_0 and the entropy generation rate in each component. Since obtaining this rate does not depend on exergy considerations, only on entropy, the exergy destruction rate becomes directly proportional to the adopted T_0.

In the context of Definition 2, considering that both the net exergies of the evaporator and condenser waters comprise the exergy input of the ORC is analogous to considering that, in a conventional ORC (which operates at temperatures above air temperature), the exergy loss in its condenser is treated as part of the cycle's exergy input, added to the exergy from the primary heat source (solar, geothermal, etc.). Moreover, for any power system based on a thermodynamic cycle, some exergy loss is associated with its operation, which does not occur in Definition 2.

Figure 6: Parametric curves as a function of (a) T_0, (b) *CR* or *PR*, and (c) P_1 for the Stirling and Ericsson cycles

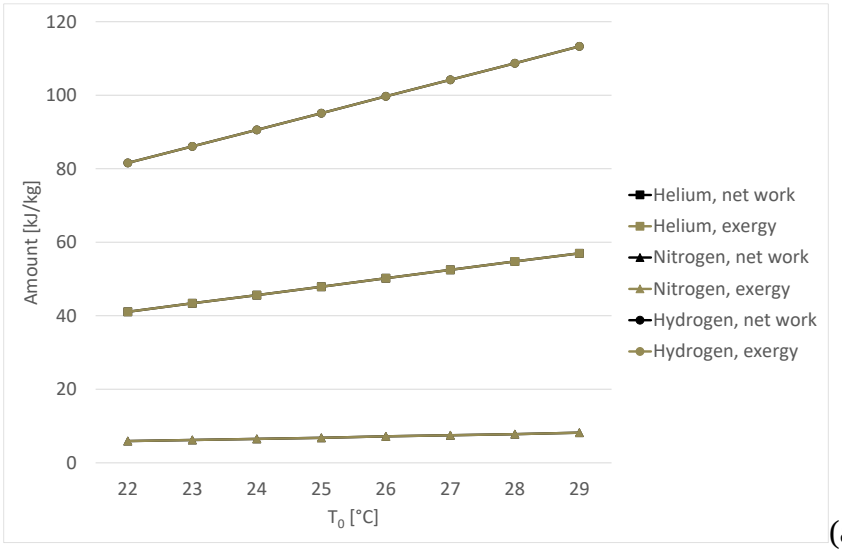

(a)

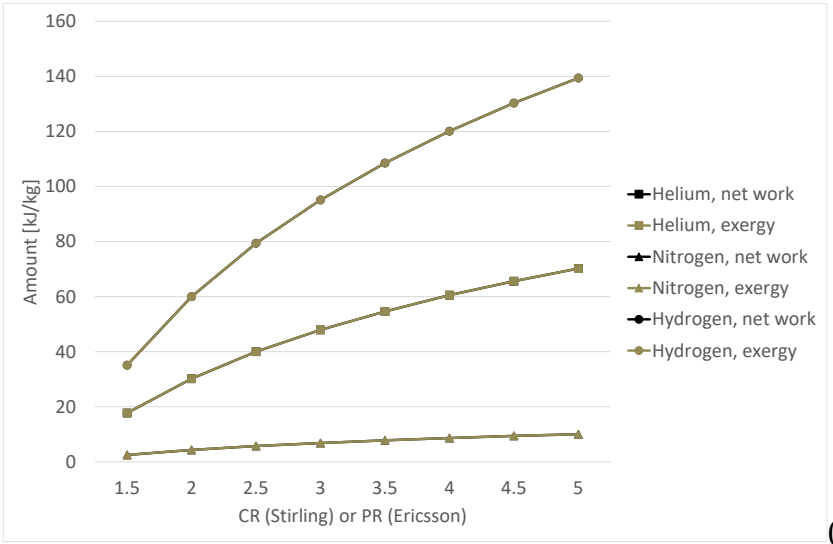

(b)

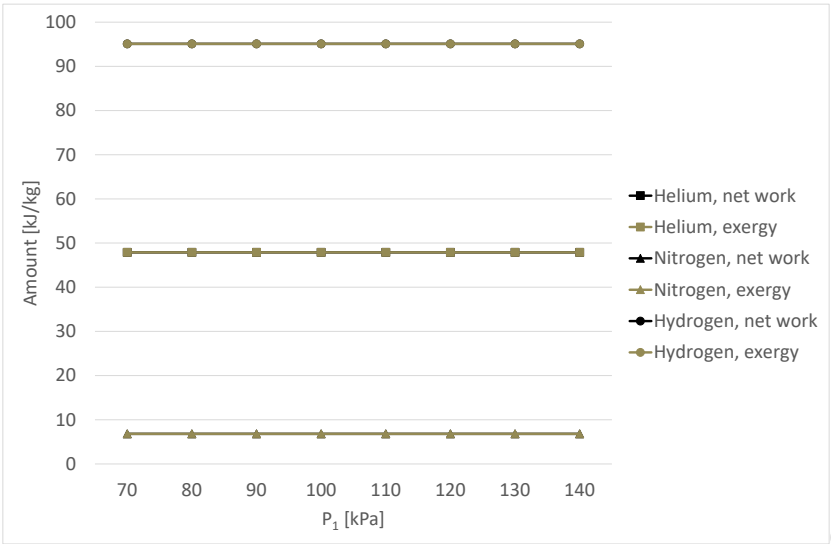

(c)

Source: The author.

Table 6: Pressures and temperatures of R-134a

Stream	State	Reference study		Present study		Deviation	
		P [kPa]	T [°C]	P [kPa]	T [°C]	P [%]	T [%]
1	Saturated vapor	631.09	23.24	631.57	23.24	0.08	≈ 0.00
2	Superheated vapor	435.78	11.73	436.07	11.72	0.07	-0.09
3	Saturated liquid	435.78	11.50	436.07	11.50	0.07	≈ 0.00
4	Compressed liquid	631.09	11.67	631.57	11.67	0.08	≈ 0.00

Source: The author.

Table 7: Mass flow rates, specific enthalpies, and specific entropies of R-134a and water

Stream	ṁ [kg/s]	h [kJ/kg]	s [kJ/kg-K]	Stream	ṁ [kg/s]	h [kJ/kg]	s [kJ/kg-K]
1	7.117	263.28	0.9212	wi	93.09	117.37	0.4091
2		257.21	0.9265	wo		102.43	0.3592
3		67.50	0.2601	ci	56.12	16.81	0.0611
4		67.75	0.2604	co		40.87	0.1470

Source: The author.

The exergy balance sheets for the three definitions are shown in Table 8. The total exergy input must be equal to the sum of the net power and the exergy destructions and losses. The percentages in parentheses are associated with exergetic efficiency and exergy destructions and losses. It is clearly seen that the results generated by the three definitions are different.

Table 8: Exergy balance sheets for Definitions 1, 2, and 3

	Amounts		
	Definition 1	Definition 2	Definition 3
Exergy input			
Evaporator	---	31.60 kW	103.30 kW
Condenser	101.95 kW	60.60 kW	---
Total	101.95 kW	92.20 kW	103.30 kW
Net power	36.84 kW (36.13%)	36.84 kW (39.95%)	36.84 kW (35.66%)
Exergy destruction			
Evaporator	16.33 kW (16.02%)	15.86 kW (17.20%)	15.03 kW (14.55%)
Turbine	15.75 kW (15.45%)	15.42 kW (16.73%)	14.84 kW (14.36%)
Condenser	23.79 kW (23.34%)	23.11 kW (25.07%)	21.90 kW (21.20%)
Pump	0.98 kW (0.96%)	0.97 kW (1.05%)	0.92 kW (0.90%)
Exergy loss			
Evaporator	8.26 kW (8.10%)	---	---
Condenser	---	---	13.77 kW (13.33%)
Total	101.95 kW	92.20 kW	103.30 kW

Source: The author.

Regardless of the adopted definition, the net power is the same. This is expected since the power generated by the ORC is obtained through the energy modeling of the cycle, which does not depend on second law considerations.

For all ORC components, the exergy destruction rates decrease as T_0 decreases. This is also expected, as it is consistent with

the Gouy-Stodola theorem. The exergy destruction rate can be calculated as the product of T_0 and the entropy generation rate in each component. Since obtaining this rate does not depend on exergy considerations, only on entropy, the exergy destruction rate becomes directly proportional to the adopted T_0.

In the context of Definition 2, considering that both the net exergies of the evaporator and condenser waters comprise the exergy input of the ORC is analogous to considering that, in a conventional ORC (which operates at temperatures above air temperature), the exergy loss in its condenser is treated as part of the cycle's exergy input, added to the exergy from the primary heat source (solar, geothermal, etc.). Moreover, for any power system based on a thermodynamic cycle, some exergy loss is associated with its operation, which does not occur in Definition 2.

Regarding Definition 3, considering the net exergy of the condenser water as an exergy loss is analogous to treating the exergy of the primary source in a conventional ORC as the exergy loss associated with the evaporator. Furthermore, considering the net exergy of the evaporator water as the cycle's exergy input is analogous, once again in a conventional ORC, to considering that the exergy of the condenser's cooling fluid is associated with the exergy input.

In summary, Definitions 2 and 3 do not make sense from an engineering perspective. On the other hand, Definition 1 is logical: by considering the net exergy of the condenser water as the exergy input of the ORC, it corresponds to the effort and cost involved in obtaining the deep cold water. This is analogous to a conventional ORC, where it reflects the effort and cost of obtaining geothermal water/steam, concentrating solar heat, etc. Moreover, considering the net exergy of the evaporator water as an exergy loss is analogous to the exergy loss in a conventional ORC's condenser: in the first case, the evaporator water is discharged into ocean water at the surface water temperature; in the second case, the exergy of the condenser's cooling fluid is dissipated into the surrounding air.

For the parametric analysis based on Definition 1, the respective pinch points of the evaporator and condenser, as well as the isentropic efficiencies of the turbine and pump, are taken into account. The effect of these parameters on the exergy destruction rate and the exergy destruction fraction is analyzed.

Figure 7 presents the parametric curves for the four parameters, with one for each component of the ORC. It is known that higher pinch points are associated with higher finite temperature differences in heat exchangers. It is also known that lower isentropic efficiencies are associated with higher amounts of friction in machines. From basic thermodynamics, the higher the amounts of irreversibility causes, the higher the rates of entropy generation. Thus, the rates of exergy destruction are also higher, whether in absolute or relative terms, with the latter represented by the exergy destruction fractions. Therefore, Definition 1 demonstrates thermodynamic robustness in light of the parametric analysis.

Whether for reversible power cycles or for the ORC, adopting the reference environment temperature as the local physical environment temperature is an approach recommended by widely accepted texts. For example, in Bejan et al. (1996), the following reasoning can be found: "If the system uses atmospheric air, for example, T_0 would be specified as the average air temperature. If both air and water from the natural surroundings are used, T_0 would be specified as the lower of the average temperatures for air and water." Following this reasoning, the (average) temperature of the warm surface water used in an OTEC system should be the reference environment temperature for the analysis of such a system. This idea is also presented in Dincer and Rosen (2021): "The environment is often modeled as a reference environment similar to the actual environment in which a system or flow

exists. This ability to tailor the reference environment to match the actual local environment is often an advantage of exergy analysis."

Therefore, the proposed standard is robust from a thermodynamic perspective, coherent from an engineering viewpoint, and compatible with statements found in established texts. The standard proposed in this work can contribute to the systematic advancement of scientific knowledge regarding OTEC systems by facilitating the comparison of exergy analysis results of different systems.

Figure 7: Parametric curves for the ORC components: (a) evaporator, (b) condenser, (c) pump, (d) turbine

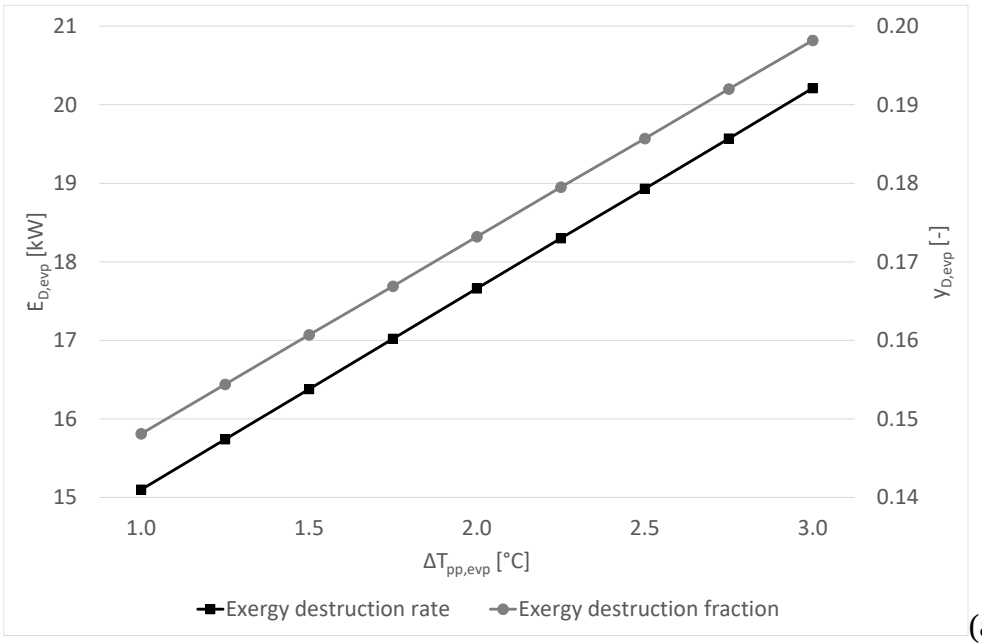

(a)

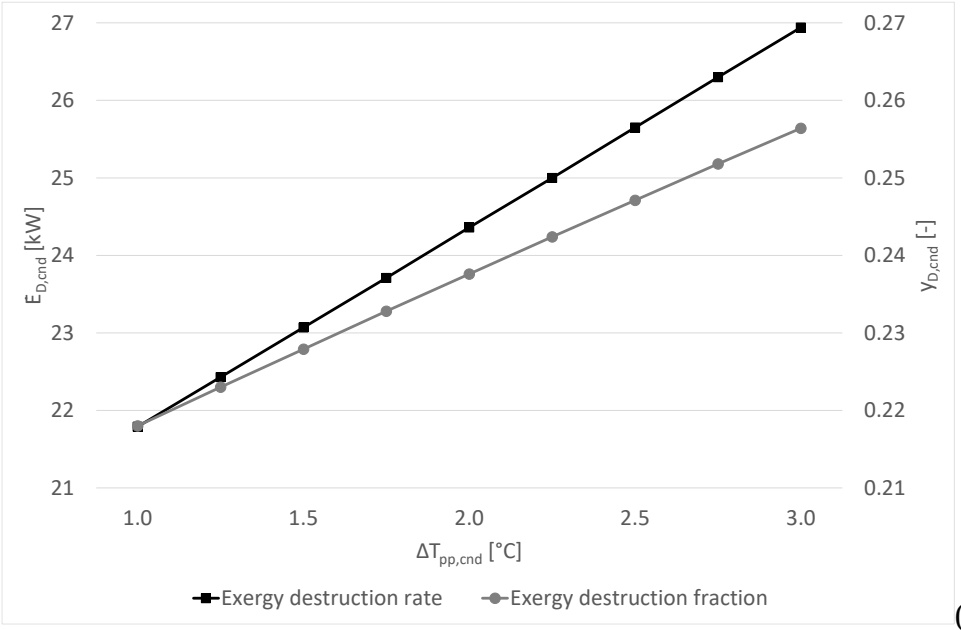

(b)

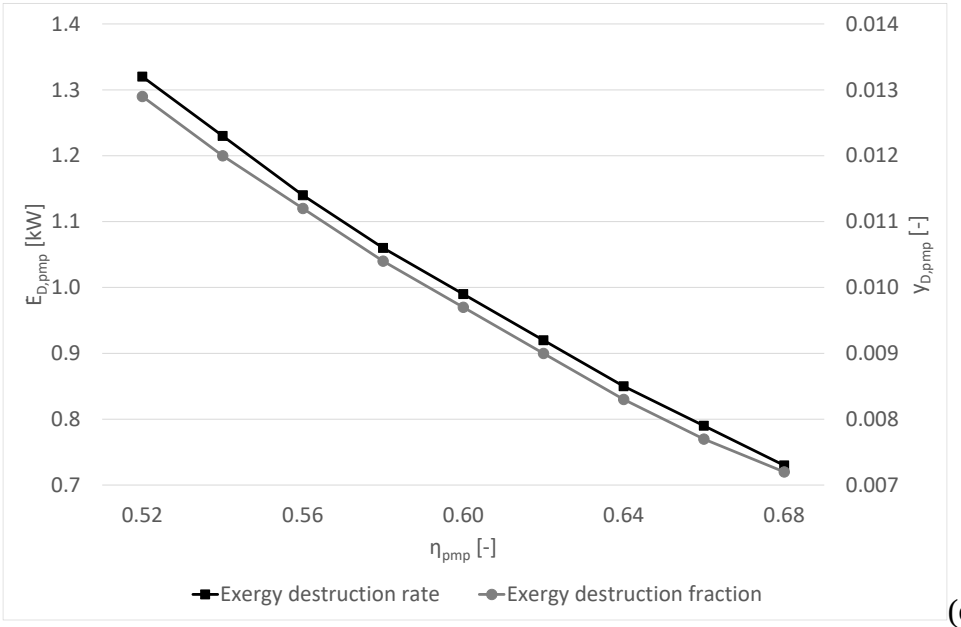

(c)

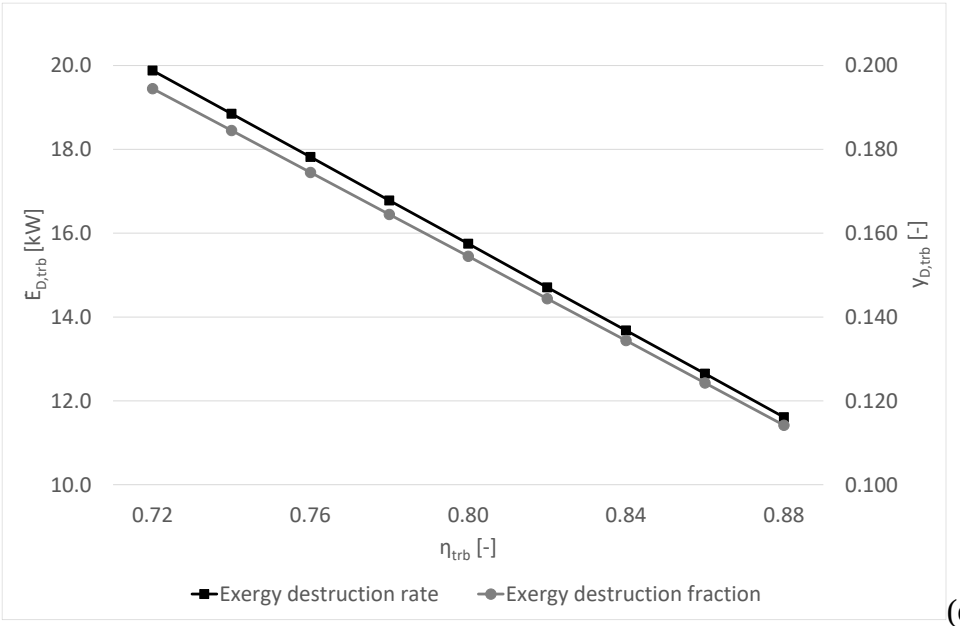

(d)

Source: The author.

4 CONCLUSION & PERSPECTIVES

In this work, a data collection was conducted on the application of exergy analysis for OTEC systems. A standard for exergy analysis of thermodynamic power cycles for OTEC was also proposed and evaluated. The main conclusions of this work are:

- Published works on the exergy analysis of OTEC systems do not follow a standard. Thus, the comparison between the results of different studies is weakened.
- For any reversible power cycle operating between T_W and T_C, where $T_W = T_0$, the work generated by the cycle is equal to the exergy associated with the heat transfer related to T_C.
- For an ORC, setting T_0 equal to the temperature of the warm surface water and considering the exergy

input as the change in exergy of the deep cold water yields robust, coherent, and compatible results with engineering thermodynamics.

The proposed standard can be applied to integrated systems that generate other products in addition to power, such as cooling and/or desalinated water. Furthermore, exergoeconomic and/or exergoenvironmental analyses of these systems can also be developed in a standardized manner.

ACKNOWLEDGMENTS

No funds, grants, or other support was received.

REFERENCES

Ahmadi, Pouria, Ibrahim Dincer, and Marc A. Rosen. 2013. "Energy and Exergy Analyses of Hydrogen Production via Solar-Boosted Ocean Thermal Energy Conversion and PEM Electrolysis." *International Journal of Hydrogen Energy* 38 (4): 1795–1805. https://doi.org/10.1016/j.ijhydene.2012.11.025.

———. 2015. "Multi-Objective Optimization of an Ocean Thermal Energy Conversion System for Hydrogen Production." *International Journal of Hydrogen Energy* 40 (24): 7601–8. https://doi.org/10.1016/j.ijhydene.2014.10.056.

Assareh, Ehsanolah, Mohammad Assareh, Seyed Mojtaba Alirahmi, Saeid Jalilinasrabady, Ali Dejdar, and Mohsen Izadi. 2021. "An Extensive Thermo-Economic Evaluation and Optimization of an Integrated System Empowered by Solar-Wind-Ocean Energy Converter for Electricity Generation – Case Study: Bandar Abas, Iran." *Thermal Science and Engineering Progress* 25 (October):100965. https://doi.org/10.1016/j.tsep.2021.100965.

Azhar, Muhammad Shuja, Ghaus Rizvi, and Ibrahim Dincer. 2017. "Integration of Renewable Energy Based Multigeneration System with Desalination." *Desalination* 404 (February):72–78. https://doi.org/10.1016/j.desal.2016.09.034.

Bahari, Mehran, Yasaman Akbari, Niloufar Akbari, Mohsen Jafari, Sajad Qezelbigloo, Rahim Zahedi, and Hossein Yousefi. 2024. "Techno-Economic Analysis and Optimization of a Multiple Green Energy Generation System Using Hybrid Wind, Solar, Ocean and Thermoelectric Energy." *Energy Systems*, June. https://doi.org/10.1007/s12667-024-00681-9.

Basta, Giuseppe, Nicoletta Meloni, Francesco Poli, Lorenzo Talluri, and Giampaolo Manfrida. 2021. "Energy, Exergy and Exergo-Economic Analysis of an OTEC Power Plant Utilizing Kalina Cycle." *Global Journal of Energy Technology Research Updates* 8 (December):1–18. https://doi.org/10.15377/2409-5818.2021.08.1.

Bejan, Adrian, George Tsatsaronis, and Michael Moran. 1996. *Thermal Design and Optimization*. New York: Wiley. https://www.wiley.com/en-us/Thermal+Design+and+Optimization-p-9780471584674.

Bernardoni, C., M. Binotti, and A. Giostri. 2019. "Techno-Economic Analysis of Closed OTEC Cycles for Power Generation." *Renewable Energy* 132 (March):1018–33. https://doi.org/10.1016/j.renene.2018.08.007.

Çengel, Yunus, Michael Boles, and

Mehmet Kanoglu. 2023. *Thermodynamics: An Engineering Approach*. 10th ed. McGraw-Hill. https://www.mheducation.com/highered/product/thermodynamics-engineering-approach-cengel-boles/M9781266664489.html.

Chen, Fengyun, Liang Zhang, Weimin Liu, Lei Liu, and Jingping Peng. 2016. "Thermodynamic Analysis of Rankine Cycle in Ocean Thermal Energy Conversion." *International Journal of Simulation: Systems, Science & Technology*, January. https://doi.org/10.5013/IJSSST.a.17.13.07.

Chu, Peter C., and Chenwu Fan. 2020. "World Ocean Thermocline Weakening and Isothermal Layer Warming." *Applied Sciences* 10 (22): 8185. https://doi.org/10.3390/app10228185.

Colorado-Garrido, Dario, Emmanuel Mendoza-Bernal, Lili M. Toledo-Paz, and Beatris A. Escobedo-Trujillo. 2024. "An Ocean Thermal Energy Conversion Power Plant: Advanced Exergy Analysis and Experimental Validation." *Renewable Energy* 223 (March):120018. https://doi.org/10.1016/j.renene.2024.120018.

Costa, Rui, and Brendan MacDonald. 2018. "Comparison of the Net Work Output between Stirling and Ericsson Cycles." *Energies* 11 (3): 670. https://doi.org/10.3390/en11030670.

Dezhdar, Ali, Ehsanolah Assareh, Sajjad Keykhah, Ali Bedakhanian, and Moonyong Lee. 2023. "A Transient Model for Clean Electricity Generation Using Solar Energy and Ocean Thermal Energy Conversion (OTEC) - Case Study: Karkheh Dam - Southwest Iran." *Energy Nexus* 9 (March):100176. https://doi.org/10.1016/j.nexus.2023.100176.

Dincer, İbrahim, and Marc A. Rosen. 2021. *Exergy: Energy, Environment and Sustainable Development*. 3rd ed. Elsevier. https://doi.org/10.1016/C2016-0-02067-3.

Doorga, Jay Rovisham Singh, Oomarsing Gooroochurn, Beenesh Anand Motah, Vimal Ramchandur, and Shane Sunassee. 2018. "A Novel Modelling Approach to the Identification of Optimum Sites for the Placement of Ocean Thermal Energy Conversion (OTEC) Power Plant: Application to the Tropical Island Climate of Mauritius." *International Journal of Energy and Environmental Engineering* 9 (4): 363–82. https://doi.org/10.1007/s40095-018-0278-4.

Du, Yanlian, Hao Peng, Jiahua Xu, Zhen Tian, Yuan Zhang, Xuanhe Han, and Yijun Shen. 2024. "Performance Analysis of Ocean Thermal Energy Conversion System Integrated with Waste Heat Recovery from Offshore Oil and Gas Platform." *Case Studies in Thermal Engineering* 54 (February):104027. https://doi.org/10.1016/j.csite.2024.104027.

F-Chart Software. 2017. "Engineering Equation Solver - EES." F-Chart Software. http://www.fchart.com.

Fachina, Vicente. 2016. "Sustainable Freshwater from the Tropical Oceans." *Journal of the Brazilian Society of Mechanical Sciences and Engineering* 38 (4): 1269–77. https://doi.org/10.1007/s40430-015-0383-8.

Fan, Chengcheng, Chengbin Zhang, and Wei Gao. 2024. "Improving the Ocean Thermal Energy Conversion by Solar Pond." *Solar Energy* 274 (May):112583. https://doi.org/10.1016/j.solener.2024.112583.

Gao, Wenzhong, Fei Wang, Zhen Tian, and

Yuan Zhang. 2024. “Experimental Investigation on the Performance of a Solar-Ocean Thermal Energy Conversion System Based on the Organic Rankine Cycle.” *Applied Thermal Engineering* 245 (May):122776. https://doi.org/10.1016/j.applthermaleng.2024.122776.

Geng, Donghan, and Xiangjie Gao. 2023. “Thermodynamic and Exergoeconomic Optimization of a Novel Cooling, Desalination and Power Multigeneration System Based on Ocean Thermal Energy.” *Renewable Energy* 202 (January):17–39. https://doi.org/10.1016/j.renene.2022.11.088.

Haroon, Muhammad, Abubakr Ayub, Nadeem Ahmed Sheikh, Muhammad Ahmed, and Al-Bara Shalaby. 2022. “Harnessing Ocean Thermal Energy from Offshore Locations in Pakistan Using an Organic Rankine Cycle.” In *ICAME-22*, 24. Basel Switzerland: MDPI. https://doi.org/10.3390/engproc2022023024.

Hasan, A., and I. Dincer. 2020. “An Ocean Thermal Energy Conversion Based System for District Cooling, Ammonia and Power Production.” *International Journal of Hydrogen Energy* 45 (32): 15878–87. https://doi.org/10.1016/j.ijhydene.2020.03.173.

Hernández-Romero, Ilse María, Fabricio Nápoles-Rivera, Antonio Flores-Tlacuahuac, and Luis Fabián Fuentes-Cortés. 2020. “Optimal Design of the Ocean Thermal Energy Conversion Systems Involving Weather and Energy Demand Variations.” *Chemical Engineering and Processing - Process Intensification* 157 (November):108114. https://doi.org/10.1016/j.cep.2020.108114.

Hoseinzadeh, Siamak, Mehdi Asadi PaeinLamouki, and Davide Astiaso Garcia. 2024. “Thermodynamic Analysis of Heat Storage of Ocean Thermal Energy Conversion Integrated with a Two-Stage Turbine by Thermal Power Plant Condenser Output Water.” *Journal of Energy Storage* 84 (April):110818. https://doi.org/10.1016/j.est.2024.110818.

Hoseinzadeh, Siamak, Ehsanolah Assareh, Amjad Riaz, Moonyong Lee, and Davide Astiaso Garcia. 2023. “Ocean Thermal Energy Conversion (OTEC) System Driven with Solar-Wind Energy and Thermoelectric Based on Thermo-Economic Analysis Using Multi-Objective Optimization Technique.” *Energy Reports* 10 (November):2982–3000. https://doi.org/10.1016/j.egyr.2023.09.131.

Huo, Erguang, Wei Chen, Zilong Deng, Wei Gao, and Yongping Chen. 2023. “Thermodynamic Analysis and Optimization of a Combined Cooling and Power System Using Ocean Thermal Energy and Solar Energy.” *Energy* 278 (September):127956. https://doi.org/10.1016/j.energy.2023.127956.

Ishaq, H., and I. Dincer. 2020. “A Comparative Evaluation of OTEC, Solar and Wind Energy Based Systems for Clean Hydrogen Production.” *Journal of Cleaner Production* 246 (February):118736. https://doi.org/10.1016/j.jclepro.2019.118736.

Ishaq, Haris, Osamah Siddiqui, and Ibrahim Dincer. 2019. “Design and Analysis of a Novel Integrated Wind-Solar-OTEC Energy System for Producing Hydrogen, Electricity, and Fresh Water.” *Journal of Solar Energy Engineering* 141 (6). https://doi.org/10.1115/1.4044023.

Jung, Jung-Yeul, Ho Saeng Lee, Hyeon-Ju Kim, Yungpil Yoo, Woo-Young Choi, and Ho-Young Kwak. 2016. “Thermoeconomic Analysis of an Ocean Thermal Energy Conversion Plant.” *Renewable Energy* 86 (February):1086–94.

https://doi.org/10.1016/j.renene.2015.09.031.

Katooli, Mohammad Hadi, Reza Askari Moghadam, and Mazdak Hooshang. 2020. "Investigation on Effective Operating Variables in Gamma-Type Stirling Engine Performance: A Simulation Approach." *SN Applied Sciences* 2 (4): 725. https://doi.org/10.1007/s42452-020-2526-5.

Khanmohammadi, Shoaib, Mohammad Mehdi Baseri, Pouria Ahmadi, Abdullah A.A.A. Al-Rashed, and Masoud Afrand. 2020. "Proposal of a Novel Integrated Ocean Thermal Energy Conversion System with Flat Plate Solar Collectors and Thermoelectric Generators: Energy, Exergy and Environmental Analyses." *Journal of Cleaner Production* 256 (May):120600. https://doi.org/10.1016/j.jclepro.2020.120600.

Khosravi, A., Sanna Syri, M.E.H. Assad, and M. Malekan. 2019. "Thermodynamic and Economic Analysis of a Hybrid Ocean Thermal Energy Conversion/Photovoltaic System with Hydrogen-Based Energy Storage System." *Energy* 172 (April):304–19. https://doi.org/10.1016/j.energy.2019.01.100.

Kim, Jun-Seong, Do-Yeop Kim, Ho-Keun Kang, and You-Taek Kim. 2017. "Performance Analysis of an Orgarnic Rankine Cycle for a Solar-Boosted Ocean Thermal Energy Conversion System According to Working Fluids." *Journal of the Korean Society of Marine Engineering* 41 (5): 402–8. https://doi.org/10.5916/jkosme.2017.41.5.402.

Langer, Jannis, Carlos Infante Ferreira, and Jaco Quist. 2022. "Is Bigger Always Better? Designing Economically Feasible Ocean Thermal Energy Conversion Systems Using Spatiotemporal Resource Data." *Applied Energy* 309 (March):118414. https://doi.org/10.1016/j.apenergy.2021.118414.

Ma, Qingfen, Xin Feng, Jingru Li, Zhongye Wu, Hui Lu, Hongfeng Luo, Chengpeng Wang, Shenghui Wang, Jie Huang, and Omid Mahian. 2024. "An Innovative Ocean Thermal Energy Conversion System with Zeotropic Rankine Cycle and Direct Contact Membrane Distillation for Enhanced Efficiency and Sustainability." *Energy* 291 (March):130349. https://doi.org/10.1016/j.energy.2024.130349.

Ma, Qingfen, Yun Zheng, Hui Lu, Jingru Li, Shenghui Wang, Chengpeng Wang, Zhongye Wu, Yijun Shen, and Xuejin Liu. 2022. "A Novel Ocean Thermal Energy Driven System for Sustainable Power and Fresh Water Supply." *Membranes* 12 (2): 160. https://doi.org/10.3390/membranes12020160.

Malik, Muhammad Zeeshan, Farayi Musharavati, Shoaib Khanmohammadi, Mohammad M. Baseri, P. Ahmadi, and Dinh Duc Nguyen. 2020. "Ocean Thermal Energy Conversion (OTEC) System Boosted with Solar Energy and TEG Based on Exergy and Exergo-Environment Analysis and Multi-Objective Optimization." *Solar Energy* 208 (September):559–72. https://doi.org/10.1016/j.solener.2020.07.049.

Moran, Michael J., Howard N. Shapiro, Daisie D. Boettner, and Margaret B. Bailey. 2018. *Fundamentals of Engineering Thermodynamics*. 9th ed. Wiley. https://www.wiley.com/en-us/Fundamentals+of+Engineering+Thermodynamics%2C+9th+Edition-p-9781119391388.

Ofosu-Adarkwa, Jeffrey, and Tang Hao. 2017. "Energy and Exergy Analysis of a

Cogeneration Cycle, Driven by Ocean Thermal Energy Conversion (OTEC)." *The International Journal of Engineering and Science* 6 (3): 32–41. https://www.theijes.com/papers/vol6-issue3/Version-2/F0603023241.pdf.

Oliveira Junior, Silvio de. 2013. *Exergy: Production, Cost and Renewability*. Green Energy and Technology. London: Springer London. https://doi.org/10.1007/978-1-4471-4165-5.

Soyturk, Gamze, and Onder Kizilkan. 2024. "An Innovative OTEC and PV/T-Based Multi-Generation System with LNG Cold Energy Recovery for Sustainable Production of Hydrogen and Distilled Water." *International Journal of Hydrogen Energy* 75 (July):613–24. https://doi.org/10.1016/j.ijhydene.2024.04.022.

Sun, Faming, Yasuyuki Ikegami, Baoju Jia, and Hirofumi Arima. 2012. "Optimization Design and Exergy Analysis of Organic Rankine Cycle in Ocean Thermal Energy Conversion." *Applied Ocean Research* 35 (March):38–46. https://doi.org/10.1016/j.apor.2011.12.006.

Sun, Qingxuan, Jiangfeng Wang, Pan Zhao, and Yiping Dai. 2017. "Thermoeconomic Analysis and Optimization of a Reverse Osmosis Desalination System Driven by Ocean Thermal Energy and Solar Energy." *Desalination and Water Treatment* 77 (May):194–205. https://doi.org/10.5004/dwt.2017.20772.

Talluri, Lorenzo, Giampaolo Manfrida, and Lorenzo Ciappi. 2021. "Exergo-Economic Assessment of OTEC Power Generation." Edited by U. Desideri, L. Ferrari, and J. Yan. *E3S Web of Conferences* 238 (February):01015. https://doi.org/10.1051/e3sconf/202123801015.

Tian, Zhen, Xianzhi Zou, Yuan Zhang, Wenzhong Gao, Wu Chen, and Hao Peng. 2023. "4E Analyses and Multi-Objective Optimization for an Innovative Solar-Ocean Thermal Energy Conversion/Air Conditioning System." *Journal of Cleaner Production* 414 (August):137532. https://doi.org/10.1016/j.jclepro.2023.137532.

Vega, Luis A. 2012. "Ocean Thermal Energy Conversion." In *Encyclopedia of Sustainability Science and Technology*, 7296–7328. New York, NY: Springer New York. https://doi.org/10.1007/978-1-4419-0851-3_695.

Wang, Meng, Rui Jing, Haoran Zhang, Chao Meng, Ning Li, and Yingru Zhao. 2018. "An Innovative Organic Rankine Cycle (ORC) Based Ocean Thermal Energy Conversion (OTEC) System with Performance Simulation and Multi-Objective Optimization." *Applied Thermal Engineering* 145 (December):743–54. https://doi.org/10.1016/j.applthermaleng.2018.09.075.

Xiao, Chenglong, and Raza Gulfam. 2023. "Opinion on Ocean Thermal Energy Conversion (OTEC)." *Frontiers in Energy Research* 11 (February). https://doi.org/10.3389/fenrg.2023.1115695.

Xiao, Chenglong, Zheng Hu, Yongping Chen, and Chengbin Zhang. 2024. "Thermodynamic, Economic, Exergoeconomic Analysis of an Integrated Ocean Thermal Energy Conversion System." *Renewable Energy* 225 (May):120194. https://doi.org/10.1016/j.renene.2024.120194.

Yang, Xiaowei, Yanjun Liu, Yun Chen, and Li Zhang. 2022. "Optimization Design of the Organic Rankine Cycle for an Ocean Thermal Energy Conversion System." *Energies* 15 (18): 6683. https://doi.org/10.3390/en15186683.

Yasunaga, Takeshi, Kevin Fontaine, and Yasuyuki Ikegami. 2021. “Performance Evaluation Concept for Ocean Thermal Energy Conversion toward Standardization and Intelligent Design.” *Energies* 14 (8): 2336. https://doi.org/10.3390/en14082336.

Yasunaga, Takeshi, and Yasuyuki Ikegami. 2020. “Finite-Time Thermodynamic Model for Evaluating Heat Engines in Ocean Thermal Energy Conversion.” *Entropy* 22 (2): 211. https://doi.org/10.3390/e22020211.

Yasunaga, Takeshi, Taisei Nakamura, Tomoya Okuno, and Yasuyuki Ikegami. 2021. “EXERGETIC PERFORMANCE EVALUATION OF OCEAN THERMAL ENERGY CONVERSION SYSTEM WITH CROSSFLOW PLATE HEAT EXCHANGERS.” In *6th International Seminar on ORC Power Systems*, ID: 87. Munich, Germany. https://mediatum.ub.tum.de/doc/1633113/6kbluhn54vbsvijrqfk4e5n7u.pdf.

Yilmaz, Fatih. 2019. “Energy, Exergy and Economic Analyses of a Novel Hybrid Ocean Thermal Energy Conversion System for Clean Power Production.” *Energy Conversion and Management* 196 (September):557–66. https://doi.org/10.1016/j.enconman.2019.06.028.

Yilmaz, Fatih, Murat Ozturk, and Resat Selbas. 2018. “Thermodynamic Performance Assessment of Ocean Thermal Energy Conversion Based Hydrogen Production and Liquefaction Process.” *International Journal of Hydrogen Energy* 43 (23): 10626–36. https://doi.org/10.1016/j.ijhydene.2018.02.021.

———. 2024. “Design and Performance Assessment of an OTEC Driven Combined Plant for Producing Power, Freshwater, and Compressed Hydrogen.” *International Journal of Hydrogen Energy* 58 (March):688–97. https://doi.org/10.1016/j.ijhydene.2024.01.220.

Yoon, Jung-In, Chang-Hyo Son, Dong-Il Yang, Hyeon-Uk Kim, Hyeon-Ju Kim, and Ho-Saeng Lee. 2013. “Exergy Analysis of R717 High-Efficiency OTEC Power Cycle for the Efficiency and Pressure Drop in Main Components.” *Journal of the Korea Society For Power System Engineering* 17 (5): 52–57. https://doi.org/10.9726/kspse.2013.17.5.052.

Yuan, Han, Ning Mei, and Peilin Zhou. 2014. “Performance Analysis of an Absorption Power Cycle for Ocean Thermal Energy Conversion.” *Energy Conversion and Management* 87 (November):199–207. https://doi.org/10.1016/j.enconman.2014.07.015.

Yuan, Han, Peilin Zhou, and Ning Mei. 2015. “Performance Analysis of a Solar-Assisted OTEC Cycle for Power Generation and Fishery Cold Storage Refrigeration.” *Applied Thermal Engineering* 90 (November):809–19. https://doi.org/10.1016/j.applthermaleng.2015.07.072.

Zainul, Rahadian, Ali Basem, Mohamad J. Alfaker, Pawan Sharma, Abhishek Kumar, Mohammed Al-Bahrani, Ahmed Elawady, Mohamed Abbas, Shatrudhan Pandey, and Hadi Fooladi. 2024. “Exergy, Exergoeconomic Optimization and Exergoenvironmental Analysis of a Hybrid Solar, Wind, and Marine Energy Power System: A Strategy for Carbon-Free Electrical Production.” *Heliyon*, August, e35171. https://doi.org/10.1016/j.heliyon.2024.e35171.

Zhang, Ji, Xiaomeng Zhang, Zhixiang Zhang, Peilin Zhou, Yan Zhang, and Han

Yuan. 2022. “Performance Improvement of Ocean Thermal Energy Conversion Organic Rankine Cycle under Temperature Glide Effect.” *Energy* 246 (May):123440. https://doi.org/10.1016/j.energy.2022.123440.

Zhang, Yuan, Yulu Chen, XuChang Qiu, Zhen Tian, Hao Peng, and Wenzhong Gao. 2024. “Experimental Study and Performance Comparison of a 1 KW-Class Solar-Ocean Thermal Energy Conversion System Integrated Air Conditioning: Energy, Exergy, Economic, and Environmental (4E) Analysis.” *Journal of Cleaner Production* 451 (April):142033. https://doi.org/10.1016/j.jclepro.2024.142033.

Zhang, Zhixiang, Han Yuan, and Ning Mei. 2023. “Theoretical Analysis on Extraction-Ejection Combined Power and Refrigeration Cycle for Ocean Thermal Energy Conversion.” *Energy* 273 (June):127216. https://doi.org/10.1016/j.energy.2023.127216.

Zhang, Zhixiang, Han Yuan, Suyun Yi, Yongchao Sun, Wenyi Peng, and Ning Mei. 2024. “Theoretical Analysis on Temperature-Lifting Cycle for Ocean Thermal Energy Conversion.” *Energy Conversion and Management* 300 (January):117946. https://doi.org/10.1016/j.enconman.2023.117946.

Zhou, Shihe, Xinyu Liu, Yongning Bian, and Shengqiang Shen. 2020. “Energy, Exergy and Exergoeconomic Analysis of a Combined Cooling, Desalination and Power System.” *Energy Conversion and Management* 218 (August):113006. https://doi.org/10.1016/j.enconman.2020.113006.

Zhou, Shihe, Xinyu Liu, Yin Feng, Yongning Bian, and Shengqiang Shen. 2021. “Parametric Study and Multi-Objective Optimization of a Combined Cooling, Desalination and Power System.” *DESALINATION AND WATER TREATMENT* 217:1–21. https://doi.org/10.5004/dwt.2021.26994.

Zhu, Keyu, Yongning Bian, and Yang Liu. 2022. “Explore the Influence of Intermediate Extraction on Thermodynamic Performance and Economy of Uehara Cycle.” *Journal of OTEC (Departmental Bulletin Paper)* 27:1–6. https://www.ioes.saga-u.ac.jp/jp/files/uploads/27-1.pdf.

Zoghi, Mohammad, Nasser Hosseinzadeh, Saleh Gharaie, and Ali Zare. 2024. “Energy and Exergy-Economic Performance Comparison of Wind, Solar Pond, and Ocean Thermal Energy Conversion Systems for Green Hydrogen Production.” *International Journal of Hydrogen Energy*, June. https://doi.org/10.1016/j.ijhydene.2024.06.183.

APPENDIX A

Considering all energy transfers as positive, the energy balance of a power cycle can be written as:

$$W_{cycle} = Q_W - Q_C$$

Rearranging:

$$W_{cycle} = Q_C\left(\frac{Q_W}{Q_C} - 1\right) = -Q_C\left(1 - \frac{Q_W}{Q_C}\right)$$

For reversible cycles, the statement below is true:

$$\frac{Q_W}{Q_C} = \frac{T_W}{T_C}$$

Substituting into the main expression:

$$W_{cycle} = -Q_C\left(1-\frac{T_W}{T_C}\right)$$

Since $T_W = T_0$, the desired result is obtained:

$$W_{cycle} = -Q_C\left(1-\frac{T_0}{T_C}\right) \quad \text{(A.1)}$$

It is emphasized that the negative sign indicates that the heat transfer and the associated exergy transfer occur in opposite directions.

APPENDIX B

Table B.1 presents the exergy balance sheet for the definition with $T_0 = (T_{wo} - 5°C)$ and the exergy input equal to the net exergy of the water from the evaporator.

Table B.1: Exergy balance sheet for the definition that yields inconsistent results

	Amount
Exergy input	
Evaporator	31.60 kW
Condenser	---
Total	31.60 kW
Net power	36.84 kW (116.58%)
Exergy destruction	
Evaporator	15.86 kW (50.20%)
Turbine	15.42 kW (48.81%)
Condenser	23.11 kW (73.14%)
Pump	0.97 kW (3.05%)
Exergy loss	
Evaporator	---
Condenser	60.60 kW (191.78%)
Total	152.80 kW

Source: The author.